MOLEKUL
eISSN: 2503-0310

Articles
https://doi.org/10.20884/1.jm.2023.18.2.7326

Enhanced Microwave Absorption Quality of Bio-Silica-Barium-Ferrite Composites: Interplay of Fe^{3+} and Si^{4+}

Wahyu Widanarto[1]*, Mukhtar Effendi[1], Wahyu Tri Cahyanto[1], Sib Krishna Ghoshal[2], Candra Kurniawan[3], Erfan Handoko[4], Mudrik Alaydrus[5]

[1]Department of Physics, Universitas Jenderal Soedirman, Purwokerto 53123, Indonesia
[2]Department of Physics and Laser Centre, AMORG, Faculty of Science, Universiti Teknologi Malaysia, Johor Bahru, Skudai 81310, Malaysia
[3]Research Center for Advanced Materials, BRIN, Bld. 224 Puspiptek Office Area, South Tangerang 15314, Indonesia
[4]Department of Physics, Universitas Negeri Jakarta, Jakarta 13220, Indonesia
[5]Department of Electrical Engineering, Universitas Mercu Buana, Jakarta 11650, Indonesia

*Corresponding author email: wahyu.widanarto@unsoed.ac.id

Received December 14, 2022; **Accepted** May 05, 2023; **Available online** July 20, 2023

ABSTRACT. This paper reports the improved microwave (MW) absorption characteristics of some newly prepared bio-silica-barium-ferrite composites (SBFCs) of the form (*x*)Bio-SiO_2:(80-*x*)Fe_2O_3:(20) BaO (where *x* = 0, 2, and 4 wt.%). These composites were prepared using the modified solid-state reaction method with simultaneous sintering at 800 and 1100 °C. SBFCs were studied to determine the impact of various bio-silica concentrations on their morphology, structure, magnetic properties, permittivity, permeability, and X-band reflection loss. Various SBFC thicknesses were simulated to determine the reflection loss curves. It has been established that the MW absorption capacity of the examined SBFCs may be altered by adjusting the bio-silica concentration and sample thickness.

Keywords: Bio-silica, Magnetic Properties, Permeability, Permittivity, Reflection Loss

INTRODUCTION

Compared to other ferrites with spinel and garnet structures, the barium ferrite magnetic material ($BaFe_{12}O_{19}$) with a wide crystalline anisotropic magnetic field was shown to be superior for applications in the gigahertz frequency range (Li et al., 2012; Li et al., 2013). A powerful uniaxial anisotropic magnetic field in $BaFe_{12}O_{19}$ makes it beneficial as a microwave (MW) absorbing material (Bierlich et al., 2017; Dong et al., 2014; Liu et al., 2012; Salman et al., 2016; Sun et al., 2012). Barium ferrite has outstanding MW absorption capacity due to its significant magnetic loss at the natural resonance frequency, wherein the magnetic loss is proportional to the quantity of Fe^{3+} present. Thus, the MW absorption properties can be adjusted by exchanging Fe^{3+} ions with other trivalent ions or a mix of divalent and tetravalent ions (Shi et al., 2019). One strategy to modify the anisotropic field and resonance frequency (f_r) is to replace Fe^{3+} with rare earth elements (Li et al., 2012; Sun et al., 2012). Such a strategy was very useful in improving the MW absorption capacity of various magnetic materials (Effendi et al., 2019; Widanarto et al., 2017, 2018). It also suggests that changing the dopants concentration makes it possible to modify the absorption characteristics of ferrites. However, the ever-increasing price of rare earth materials limits their broad applications. Based on these factors, we attempted to use some effective doping agent alternatives to the rare earth.

A previous study revealed that rice husk could be a valuable source of high-quality bio-silica after full burning at temperatures 800 to 1000 °C (Widanarto et al., 2020). Bio-silica derived from rice husk has various advantages over mineral silica (Malahayati et al., 2021). This silica is fine-grained, highly reactive, has cheap extraction costs because of its wide availability as raw materials, and may be used as a heavy metal binder. Considering these interesting attributes of bio-silica, the modified solid-state reaction approach was used to substitute Fe^{3+} ions in barium ferrite with Si^{4+} ions (bio-silica). The role of different bio-silica doping concentrations in improving the surface morphology, structure, composition, magnetic properties, permeability, and permittivity of the prepared bio-silica-barium-ferrite composites (SBFCs) was examined. By estimating the reflection loss (R_L) based on the transmission/reflection line theory, the MW absorption parameters of the SBFCs were determined (Kumar & Chatterjee, 2018; Meng et

al., 2015; Shi et al., 2019) that employed reflection reduction via impedance matching. The reflection loss curves were then simulated for various thicknesses of the SBFCs in which the matching thickness (t_m) depended on the resonance frequency (f_r), complex relative permeability (μ_r), and permittivity (ε_r) (Handoko et al., 2018; X. Li et al., 2018; Narang et al., 2017). In accordance with the Nicholson-Ross-Weir (NRW) approach (Ahmad et al., 2015; Soleimani et al., 2012), the complex relative permeability ($\mu_r = \mu'-j\mu''$) and permittivity ($\varepsilon_r = \varepsilon'-j\varepsilon''$) values of samples were determined using the following formulas:

$$\mu_r = \frac{1+\Gamma}{\Lambda(1-\Gamma)\sqrt{\frac{1}{\lambda_0^2}-\frac{1}{\lambda_c^2}}} \quad (1)$$

$$\frac{1}{\Lambda^2} = -\left[\frac{1}{2\pi d} ln\left(\frac{1}{T}\right)\right]^2 \quad (2)$$

$$\varepsilon_r = \frac{\lambda_0^2}{\mu_r}\left(\frac{1}{\lambda_c^2} - \left[\frac{1}{2\pi d} ln\left(\frac{1}{T}\right)\right]^2\right) \quad (3)$$

where λ_0 is the wavelength in vacuum, λ_c is the cut-off wavelength, c is the speed of light, and d is the thickness of the sample. In the meantime, the reflection loss (R_L) values were calculated using the transmission/reflection line theory (Handoko et al., 2018; Kumar & Chatterjee, 2018; Meng et al., 2015; Shi et al., 2019; Widanarto et al., 2020) as follows:

$$R_L = 20\, log\left|\frac{Z_{in}-1}{Z_{in}+1}\right| \quad (4)$$

$$Z_{in} = \sqrt{\frac{\mu_r}{\varepsilon_r}} tanh\left[-j\frac{2\pi f d}{c}\sqrt{\mu_r \varepsilon_r}\right] \quad (5)$$

where Z_{in} is the input impedance of the material and f is the MW frequency.

EXPERIMENTAL SECTION

Three SBFC (coded as SBF0, SBF2 and SBF4) of chemical composition (x) Bio-SiO_2:(80-x)Fe_2O_3:(20)BaO, (x = 0, 2 and 4 wt.%) were synthesized using the modified solid-state reaction method. Basic constituents like $BaCO_3$ powder (from Merck with 99% purity), bio-silica, and γ-Fe_2O_3 were used to prepare the proposed SBFCs. First, $BaCO_3$ powder was calcined at 350 °C for 15 minutes in the open air to remove carbon components. The rice husk ash was then sintered in a furnace at 1000 °C for three hours in ambient air to form bio-silica. During this time, Fe_3O_4 was extracted from iron sand and sintered at 850 °C for three hours to yield γ-Fe_2O_3 (Widanarto et al., 2015). The bio-silica powder was gradually blended with the γ-Fe_2O_3 and BaO powders. The powder was compressed into pellets and sintered in an air environment at 800 (for one hour) and 1100 °C (for five hours) before being cooled to room temperature by natural means. WR90 sample holder was utilized as a container for some crushed pellets to improve characterization. Finally, the crushed pellets were mixed with epoxy resin at a mass ratio of 7:3 to form a rectangular sample.

The field emission scanning electron microscope (FESEM JIB-4610F) was employed to evaluate the prepared samples' morphology and microstructure. To record the crystal structures and phases of the samples, the SmartLab (3 kW) X-ray diffractometer equipped with the Cu–Kα line of wavelength (λ) ≈ 0.1541874 nm was used. The vibrating sample magnetometer (VSM, Oxford 1.2H) was utilized to examine the magnetic characteristics of the suggested samples. Meanwhile, the scattering characteristics (S) of the specimens were measured using a vector network analyzer (VNA) from Keysight (PNA-L N5232A). The MW absorbance values of the samples were calculated to get the components of S (S_{11}, S_{12}, S_{21}, and S_{22}). The values of S_{11} and S_{21} define the coefficients of reflection (Γ) and transmission (T), respectively. The recorded values of S_{22} and S_{12} were disregarded due to their resemblance to those of S_{11} and S_{21}.

RESULTS AND DISCUSSION

Crystal Structures of SBFCs

Figure 1 presents X-ray diffraction (XRD) patterns of the as-synthesized SBFCs. In pure SBF0 samples, all detected peaks contained the $BaFe_{12}O_{19}$ (ICDD 00-039-1433) main hexagonal crystal lattice with a crystal configuration of $a = b = 0{,}5894$ nm, $c = 2{,}3215$ nm, $\alpha = \beta = 90°$ and $\gamma = 120°$. The peak at 27.52 ° is produced by the monoclinic crystalline phase of $Ba_2Fe_2O_5$ (ICDD 00-043-0256). The SBF2 composite's XRD pattern still exhibits $BaFe_{12}O_{19}$ (ICDD 00-039-1433). The SBF2 composite reveals a new barium silicate phase ($Ba_3Si_5O_{13}$) with a monoclinic crystal lattice structure (ICDD 00-026-0179). The SBF4 reveals a new phase of barium ferrite silicate $BaFeSi_4O_{10}$ (ICDD 00-003-0402). It is asserted that substituting Fe^{3+} in barium ferrite with Si^{4+} can produce a tetragonal phase of $BaFeSi_4O_{10}$.

Surface Morphology of SBFCs

Figure 2 shows a SEM micrograph of SBFCs which consists of irregular microstructure packed with hexagonal particle morphology of average size 5 μm. It is noticed that these porous composite particles adhere to one another, producing numerous intergranular pores. The replacement of Fe^{3+} by Si^{4+} (from bio-silica) in BFCs results in a new tetragonal phase of $BaFeSi_4O_{10}$. The intergranular pores of this composite particle phase are preferred to be occupied by Si^{4+} at the lattice site, providing the microstructure with increased porosity. These pores contain finer particles on the inside that are suitable for the random scattering of MW in all directions, thus favoring MW entrapment and modification of the MW absorption quality of the composites. It has been determined that the various types of surface morphology and particle distribution in SBFCs are accountable for their increased magnetic characteristics and reflection loss.

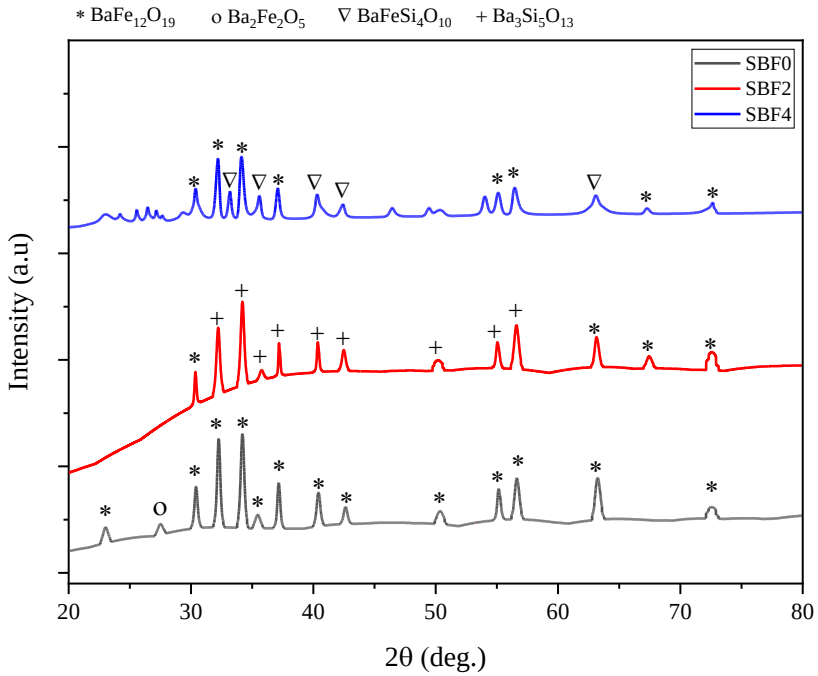

Figure 1. XRD patterns for the as-synthesized SBFCs

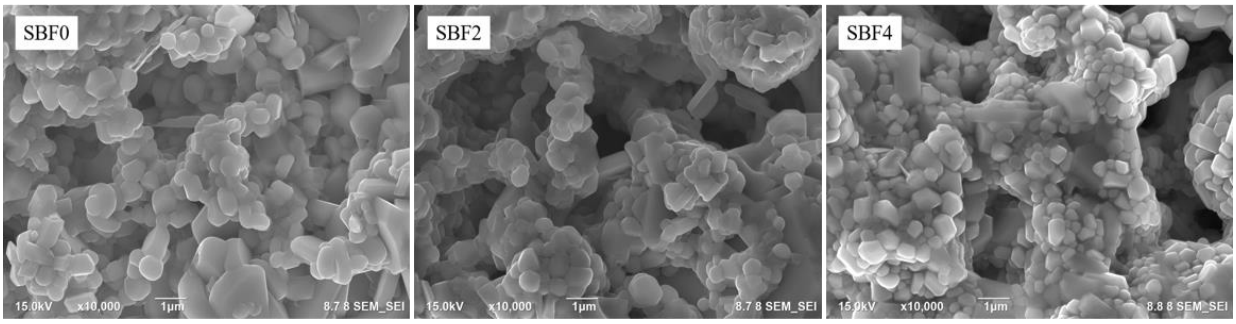

Figure 2. SEM micrograph of the as-synthesized SBFCs

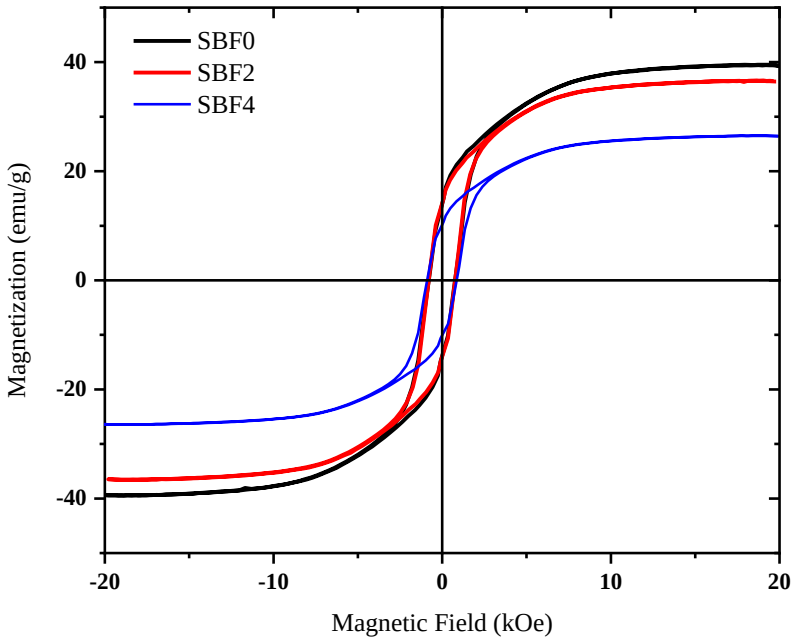

Figure 3. Room temperature hysteresis magnetic curve of the as-synthesized SBFCs

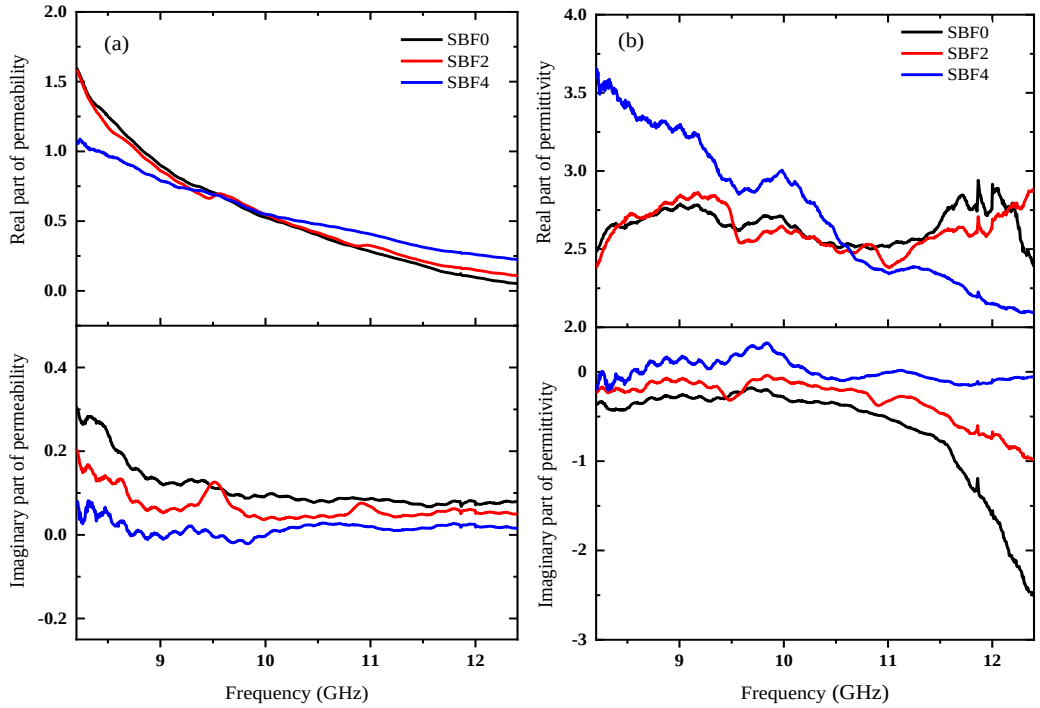

Figure 4. Frequency-dependent complex relative (**a**) permeability and (**b**) permittivity of the as-synthesized SBFCs

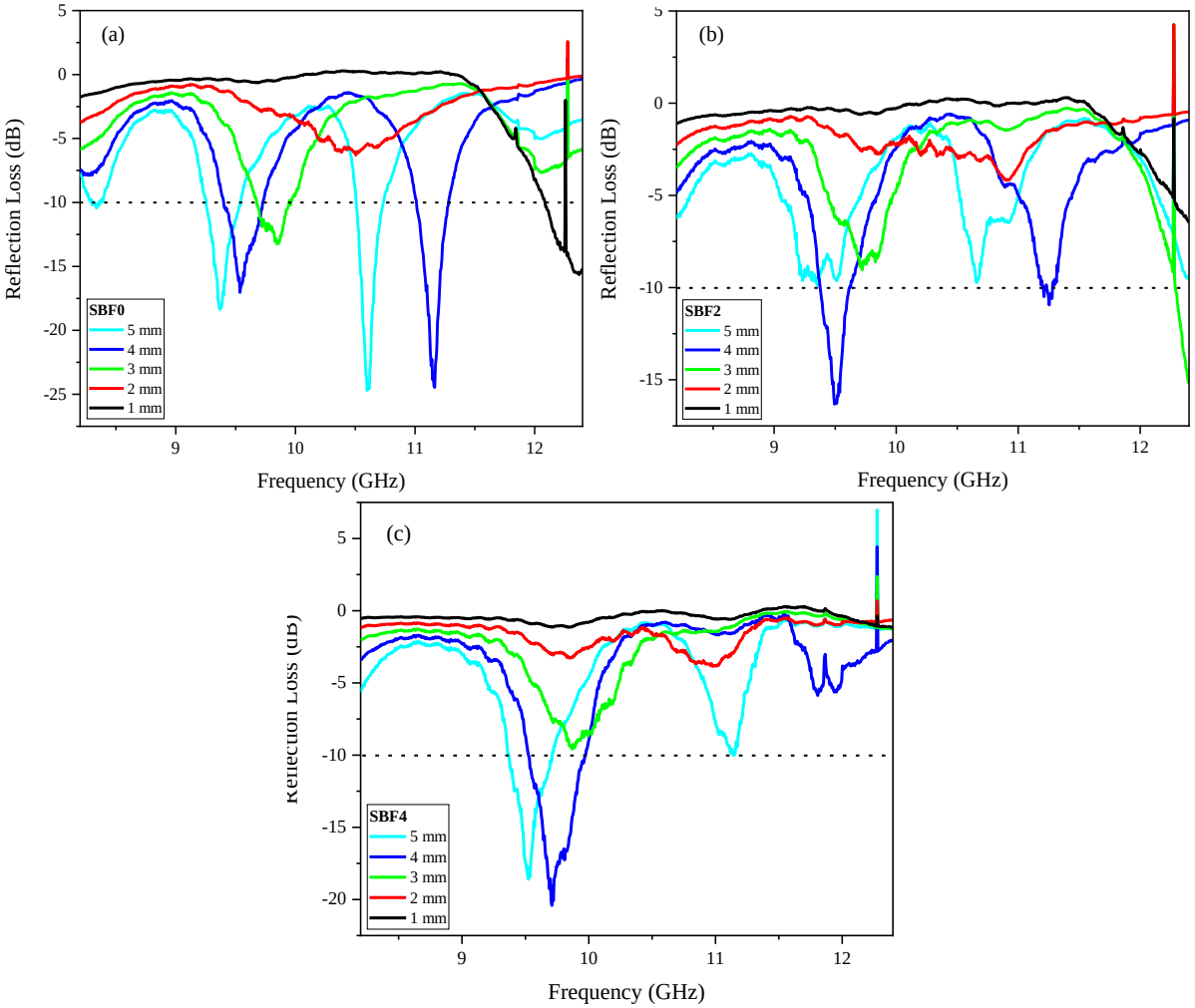

Figure 5. Frequency-dependent reflection loss of (**a**) SBF0, (**b**) SBF2, and (**c**) SBF4 with various thicknesses of 1 – 5 mm

Magnetic Properties of the as-synthesized SBFCs

Figure 3 shows the *M-H* hysteresis curve of the synthesized SBFCs at room temperature. Due to the inclusion of bio-silica into the composite, the saturation magnetization values of SBFCs are decreased from 39.5 to 26.5 emu/g. However, due to the increase in bio-silica concentration, the coercivity field values are insignificantly influenced (from 775.9 to 811.0 Oe). SBF4 samples exhibit a significant drop in saturation magnetization due to the existence of a crystalline phase of tetragonal $BaFeSi_4O_{10}$. Generally, an increase in the bio-silica content causes an enhancement of the coercive field values of SBFCs. The hysteresis loop area of SBFCs is increased from 15.9 to 31.0 kOe.emu/g with the increase of bio-silica content from 0 to 2 %. Adding bio-silica into the composites produces a reasonable change in the saturation magnetization and coercivity field values, thus altering the magnetic permeability of SBFCs. Because the magnetism in the composites is aroused from Fe^{3+}, consequently Fe^{3+} substitution with Si^{4+} is responsible for lowering Fe^{3+} quantity in the structure, modifying the complex relative permeability. The other possibility was related to the Fe^{3+} substitution by Si^{4+}-mediated ions affecting the Fe^{3+}–O–Fe^{2+} superexchange interaction in the proposed ferrites.

Complex Relative Permeability and Permittivity of the as-synthesized SBFCs

The complex relative permeability and permittivity are the two key factors that govern the loss behavior of electromagnetic wave propagation through a ferrite material (Chen et al., 2007; Kanwal et al., 2018; Korolev et al., 2012; Y. Li et al., 2017; Ozah & Bhattacharyya, 2013; Qi et al., 2019; Sun et al., 2012; Yang et al., 2019).

Due to the general polarization of the magnetic dipole at higher MW frequencies, the real part of the permeability determines the gradual decrease in magnetic energy storage capacity. With the increase of bio-silica contents from 0 to 4 wt.%, the apparent permeability values of the composites decrease from approximately 1.5 to nearly zero (for SBF0 and SBF2). Meanwhile, the imaginary part of the permeability describes the observed magnetic loss factor. The imaginary permeability values of SBF0 and SBF2 are dropped from their respective values of 0.3 and 0.2 to near zero. The relaxation process keeps it almost constant at zero for SBF4, resulting in MW dissipation energy as thermal energy. Generally, the complex permeability in the MW frequency range is related to the ferromagnetic resonance, wherein the magnetic permeability is comparable to air at frequencies more significant than the natural resonance frequency (Kanwal et al., 2018). In the present study, the magnetic permeability is found to be in the range of 1-1.5, and the loss was near zero, indicating that the ferromagnetic frequency is far lower than the observed frequency range.

The real permittivity value indicates that the composite did not absorb the energy from the applied external electric field. The SBF0 sample's real permittivity value remains stable with increasing MW frequencies, whereas the SBF4 sample declined significantly. The SBF2, on the other hand, increases in frequency over 12 GHz due to electric dipole polarization. The electrical energy dissipation ability of SBFCs is indicated by the imaginary value of the permittivity (dielectric loss factor). With increasing frequency, the imaginary permittivity values of SBF0 and SBF2 decrease gradually, meanwhile remaining stable for SBF4. The negative imaginary permittivity of SBF0 and SBF2 samples in the 8.2 to 12.4 GHz frequency range indicates electrical field energy storage rather than dissipation. Moreover, the sample's electrical dipole polarization-enabled dielectric loss factor is primarily governed by the main heating mechanism or electrical field energy dissipation as he at within the material (Widanarto et al., 2020).

Microwave Reflection Loss of the as-synthesized SBFCs

The MW frequency-dependent reflection loss (R_L) of SBFCs with varying Si^{4+} content and thickness is depicted in **Figure 5**. The R_L and bandwidth of the material prove its MW absorption capabilities. The SBF0 with 4 and 5 mm thicknesses achieves the lowest R_L values of -24.80 dB at 10.6 and 11.1 GHz frequencies. Furthermore, SBF2 with thicknesses of 1, 2, and 5 mm is higher than - 10 dB at all frequencies. At a frequency of 9.5 GHz, SBF2, with a thickness of 4 mm, has the lowest R_L value of -16.7 dB. Then, for all frequencies, SBF4 with thicknesses of 1, 2, and 3 mm are more than − 10 dB. The SBF4 with 4 and 5 mm thicknesses has the lowest R_L values of -21.2 dB at 9.7 GHz and -18 dB at 9.5 GHz, respectively. Based on this, it was demonstrated that the MW absorption capacity of SBFCs may be adjusted mainly by modifying the number of impurities or dopants (bio-silica) and sample thickness to meet X-band application demands.

CONCLUSIONS

A new bio-silica incorporated barium ferrite composites (SBFCs) was synthesized using the modified solid-state reaction method. The proposed SBFCs display improved MW absorption quality due to the interplay of Fe^{3+} and Si^{4+} in the structures. It is discovered that the surface morphology, structure, magnetic characteristics, permittivity, permeability, and MW reflection loss of the suggested SBFCs are sensitive to the substitution of Fe^{3+} with Si^{4+} in the composite matrix. In addition, the MW reflection loss of the studied SBFCs strongly depends on the sample thickness. The composite of thickness 4 mm exhibited the best performance. Most importantly, bio-silica being an abundant and cheap natural resource can be very useful for producing such good quality

environmental-friendly MW absorption candidates with enhanced properties. It is affirmed that the produced SBFCs may be beneficial for diverse MW absorption applications.

ACKNOWLEDGMENTS

The authors are grateful to the Kementerian Pendidikan, Kebudayaan, Riset dan Teknologi Republik Indonesia (Contract number: T/1425/UN23.18/PT.0l.01/2021) and UTM Malaysia (UTMFR 20H65) for their financial assistance.

REFERENCES

Ahmad, A. F., Abbas, Z., Obaiys, S. J., Ibrahim, N., & Zainuddin, M. F. (2015). Microwave characterization of bio-composites materials based finite element and Nicholson-Ross-Weir methods. *Malaysian Journal of Science*, *34*(2), 180–184. https://doi.org/10.22452/mjs.vol34no2.5

Bierlich, S., Gellersen, F., Jacob, A., & Töpfer, J. (2017). Low-temperature sintering and magnetic properties of Sc- and In-substituted M-type hexagonal barium ferrites for microwave applications. *Materials Research Bulletin*, *86*, 19–23. https://doi.org/10.1016/j.materresbull.2016.09.025

Chen, N., Mu, G., Pan, X., Gan, K., & Gu, M. (2007). Microwave absorption properties of $SrFe_{12}O_{19}/ZnFe_2O_4$ composite powders. *Materials Science and Engineering: B*, *139*(2–3), 256–260. https://doi.org/http://dx.doi.org/10.1016/j.mseb.2007.02.002

Dong, C., Wang, X., Zhou, P., Liu, T., Xie, J., & Deng, L. (2014). Microwave magnetic and absorption properties of M-type ferrite $BaCo_xTi_xFe_{12-2x}O_{19}$ in the Ka band. *Journal of Magnetism and Magnetic Materials*, *354*, 340–344. https://doi.org/10.1016/j.jmmm.2013.11.008

Effendi, M., Pratama, D. P., Cahyanto, W. T., & Widanarto, W. (2019). The effects of sintering temperature on structure, magnetic properties and microwave absorption capability of manganese-natural ferrite. *Journal of Physics: Conference Series*, *1153*(1). https://doi.org/10.1088/1742-6596/1153/1/012060

Handoko, E., Sugihartono, I., Budi, S., Randa, M., Jalil, Z., & Alaydrus, M. (2018). The effect of thickness on microwave absorbing properties of barium ferrite powder. *Journal of Physics: Conference Series*, *1080*(1). https://doi.org/10.1088/1742-6596/1080/1/012002

Kanwal, M., Ahmad, I., Meydan, T., Cuenca, J. A., Williams, P. I., Farid, M. T., & Murtaza, G. (2018). Structural, magnetic and microwave properties of gadolinium-substituted Ca-Ba M-type hexagonal ferrites. *Journal of Electronic Materials*, *47*(9), 5370–5377. https://doi.org/10.1007/s11664-018-6420-5

Korolev, K. A., McCloy, J. S., & Afsar, M. N. (2012). Ferromagnetic resonance of micro- and nano-sized hexagonal ferrite powders at millimeter waves. *Journal of Applied Physics*, *111*(7). https://doi.org/10.1063/1.3671793

Kumar, S., & Chatterjee, R. (2018). Complex permittivity, permeability, magnetic and microwave absorbing properties of Bi^{3+} substituted U-type hexaferrite. *Journal of Magnetism and Magnetic Materials*, *448*, 88–93. https://doi.org/10.1016/j.jmmm.2017.06.123

Li, C.-J., Wang, B., & Wang, J.-N. (2012). Magnetic and microwave absorbing properties of electrospun $Ba_{(1-x)}La_xFe_{12}O_{19}$ nanofibers. *Journal of Magnetism and Magnetic Materials*, *324*(7), 1305–1311. https://doi.org/10.1016/j.jmmm.2011.11.016

Li, W., Qiao, X., Li, M., Liu, T., & Peng, H. X. (2013). La and Co substituted M-type barium ferrites processed by sol-gel combustion synthesis. *Materials Research Bulletin*, *48*(11), 4449–4453. https://doi.org/10.1016/j.materresbull.2013.07.044

Li, X., Yu, L., Yu, L., Dong, Y., Gao, Q., Yang, Q., Yang, W., Zhu, Y., & Fu, Y. (2018). Chiral polyaniline with superhelical structures for enhancement in microwave absorption. *Chemical Engineering Journal*, *352*(June), 745–755. https://doi.org/10.1016/j.cej.2018.07.096

Li, Y., Wang, J., Liu, R., Zhao, X., Wang, X., Zhang, X., & Qin, G. (2017). Dependence of gigahertz microwave absorption on the mass fraction of Co@C nanocapsules in composite. *Journal of Alloys and Compounds*, *724*, 1023–1029. https://doi.org/10.1016/j.jallcom.2017.07.101

Liu, Y., Wang, T. J., Liu, Y., Li, X. J., & Liu, Y. (2012). Mechanism for synthesizing barium hexagonal ferrite by sol-gel method. *Advanced Materials Research*, *549*, 105–108. https://doi.org/10.4028/www.scientific.net/AMR.549.105

Malahayati, M., Yufita, E., Ismail, I., Mursal, M., Idroes, R., & Jalil, Z. (2021). The Effect of natural silica from rice husk ash and nickel as a catalyst on the hydrogen storage properties of MgH_2. *Journal of Ecological Engineering*, *22*(11), 79–85. https://doi.org/10.12911/22998993/142959

Meng, P., Xiong, K., Wang, L., Li, S., Cheng, Y., & Xu, G. (2015). Tunable complex permeability and enhanced microwave absorption properties of $BaNi_xCo_{1-x}TiFe_{10}O_{19}$. *Journal of Alloys and Compounds*, *628*, 75–80. https://doi.org/10.1016/j.jallcom.2014.10.163

Narang, S. B., Pubby, K., & Singh, C. (2017). Thickness and composition tailoring of K- and

Ka-band microwave absorption of BaCoxTixFe(12-2x)O19 ferrites. *Journal of Electronic Materials*, *46*(2), 718–728. https://doi.org/10.1007/s11664-016-5059-3

Ozah, S., & Bhattacharyya, N. S. (2013). Nanosized barium hexaferrite in novolac phenolic resin as microwave absorber for X-band application. *Journal of Magnetism and Magnetic Materials*, *342*. https://doi.org/10.1016/j.jmmm.2013.04.050

Qi, Z., Chunbo, L., Zhuang, W., Yang, Y., Zhiyong, X., Haikun, Z., & Chudong, C. (2019). Preparation of rGO/PVA/CIP composites and their microwave absorption properties. *Journal of Magnetism and Magnetic Materials*, *479*(September 2018), 337–343. https://doi.org/10.1016/j.jmmm.2018.11.129

Salman, S., Afghahi, S. S. S., Jafarian, M., & Atassi, Y. (2016). Microstructural and magnetic studies on $BaMg_xZn_xX_{2x}Fe_{12-4x}O_{19}$ (X=Zr,Ce,Sn) prepared via mechanical activation method to act as a microwave absorber in X-band. *Journal of Magnetism and Magnetic Materials*, *406*, 184–191. https://doi.org/10.1016/j.jmmm.2016.01.020

Shi, K., Li, J., He, S., Bai, H., Hong, Y., Wu, Y., Jia, D., & Zhou, Z. (2019). A superior microwave absorption material: Ni^{2+}-Zr^{4+} Co-Doped barium ferrite ceramics with large reflection loss and broad bandwidth. *Current Applied Physics*, *19*(7), 842–848. https://doi.org/10.1016/j.cap. 2019.03.018

Soleimani, H., Abbas, Z., Yahya, N., Soleimani, H., & Ghotbi, M. Y. (2012). Determination of complex permittivity and permeability of lanthanum iron garnet filled PVDF-polymer composite using rectangular waveguide and Nicholson–Ross–Weir (NRW) method at X-band frequencies. *Measurement*, *45*(6), 1621–1625. https://doi.org/10.1016/j.measurement.2012.02.014

Sun, C., Sun, K., & Chui, P. (2012). Microwave absorption properties of Ce-substituted M-type barium ferrite. *Journal of Magnetism and Magnetic Materials*, *324*(5), 802–805. https://doi.org/10.1016/j.jmmm.2011.09.023

Widanarto, W., Amirudin, F., Ghoshal, S. K., Effendi, M., & Cahyanto, W. T. (2017). Structural and magnetic properties of La^{3+} substituted barium−natural nanoferrites as microwave absorber in X-band. *Journal of Magnetism and Magnetic Materials*, *426*, 483–486. https://doi.org/10.1016/j.jmmm.2016.11.124

Widanarto, W., Ardenti, E., Ghoshal, S. K., Kurniawan, C., Effendi, M., & Cahyanto, W. T. (2018). Significant reduction of saturation magnetization and microwave-reflection loss in barium-natural ferrite via Nd^{3+} substitution. *Journal of Magnetism and Magnetic Materials*, *456*, 288–291. https://doi.org/10.1016/j.jmmm.2018.02.050

Widanarto, W., Effendi, M., Ghoshal, S. K., Kurniawan, C., Handoko, E., & Alaydrus, M. (2020). Bio-silica incorporated barium ferrite composites: Evaluation of structure, morphology, magnetic and microwave absorption traits. *Current Applied Physics*, *20*(5), 638–642. https://doi.org/10.1016/j.cap. 2020.02.019

Widanarto, W., Jandra, M., Ghoshal, S. K., Effendi, M., & Cahyanto, W. T. (2015). $BaCO_3$ mediated modifications in structural and magnetic properties of natural nanoferrites. *Journal of Physics and Chemistry of Solids*, *79*, 78–81. https://doi.org/10.1016/j.jpcs.2014.12.011

Yang, M., Zhou, W., Liu, Y., Li, L., Luo, F., & Zhu, D. (2019). $LiCo_xNi_{1-x}O_2$ with high dielectric and microwave absorption performance in X-band. *Ceramics International*, *45*(May), 17800. https://doi.org/10.1016/j.ceramint.2019.05.351